arXiv:0705.1448v1 [physics.optics] 10 May 2007

On convergence of the extended strong–property–fluctuation theory for bianisotropic homogenized composites

Jiajia Cui[1] and Tom G. Mackay[2]

School of Mathematics, University of Edinburgh, Edinburgh EH9 3JZ, United Kingdom.

Abstract

The strong–property–fluctuation theory (SPFT) provides a sophisticated means of estimating the effective constitutive parameters of a homogenized composite material (HCM), which takes account of the statistical distribution of the component particles. We present an extended version of the third–order SPFT in which the component particles are represented as depolarization regions of nonzero volume. Numerical results are provided for a bianisotropic homogenization scenario wherein the HCM is a Faraday chiral medium. Thereby, convergence of the extended SPFT at the second–order level of approximation is demonstrated within the long–wavelength regime.

Keywords: Depolarization region, Faraday chiral medium, Bruggeman formalism, Long–wavelength regime

PACS numbers: 83.80.Ab, 05.40.-a, 81.05.Zx

1 Introduction

Suppose that two (or more) homogeneous materials are blended together to form a composite. If the length scale of inhomogeneities in the composite is β, then the composite is inhomogeneous at wavelengths $\lesssim \beta$, but homogeneous at wavelengths $\gg \beta$ (Lakhtakia, 1996). The homogenized composite material (HCM) which arises in the long–wavelength regime may exhibit properties that are not exhibited by its component materials, or at least not exhibited to the same extent. Thus, HCMs represent prime examples of metamaterials (Walser, 2003). Interest in complex metamaterials, and HCM–based complex metamaterials in particular, has escalated in recent years, which serves to highlight the need for accurate formalisms to estimate the constitutive parameters of complex HCMs (Mackay, 2005).

The strong–property–fluctuation theory (SPFT) provides a sophisticated basis for estimating the constitutive parameters of HCMs (Tsang & Kong, 1981) which has distinct advantages over con-

[1]email: s0457353@sms.ed.ac.uk
[2]email: T.Mackay@ed.ac.uk

ventional formalisms such as those named after Maxwell Garnett and Bruggeman (Lakhtakia, 1996; Ward, 1995). This is achieved through accommodating higher–order descriptions of the distributional statistics of the component materials which are brought together to form the HCM. Indeed, in principle, the SPFT can accommodate spatial correlation functions of arbitrarily high order. However, in practice, the SPFT is usually implemented at the second–order level of approximation wherein a two–point covariance function and its associated correlation length characterize the distributional statistics of the component materials. Versions of the second–order SPFT have been developed for isotropic (Tsang & Kong, 1981; Michel & Lakhtakia, 1995), anisotropic (Genchev, 1992; Zhuck, 1994) and bianisotropic (Mackay, Lakhtakia, & Weiglhofer, 2000) linear HCMs, as well as for certain nonlinear HCMs (Lakhtakia, 2001; Mackay, Lakhtakia, & Weiglhofer, 2003; Mackay, 2003). The third–order SPFT has also been established for bianisotropic HCMs which are weakly nonlinear. Convergence at the second–order level of approximation has been established for isotropic chiral mediums, and also more generally for bianisotropic mediums which are weakly anisotropic (Mackay, Lakhtakia, & Weiglhofer, 2001a).

Commonly, in homogenization formalisms — including the SPFT — the electromagnetic responses of the component material particles are represented by depolarization dyadics. Often the depolarization dyadics are taken to correspond to vanishingly small regions; accordingly, the spatial extent of the component material particles is neglected (Michel, 1997; Michel & Weiglhofer, 1997). An extended version of the second–order SPFT has recently been established which allows for depolarization regions of nonzero volume (Cui & Mackay, 2007a). Numerical studies based on the extended SPFT have demonstrated that the depolarization contribution associated with regions of nonzero volume can have significant effects on estimates of the HCM constitutive parameters (Cui & Mackay, 2007a,b). We note that similarly extended versions of the Maxwell Garnett (Lakhtakia & Shanker, 1993; Shanker & Lakhtakia, 1993a,b) and Bruggeman (Prinkey, Lakhtakia, & Shanker, 1994; Shanker, 1996) homogenization formalisms have also been established, and the spatial extent of the component material particles has been emphasized in other homogenization studies too (Doyle, 1989; Dungey & Bohren, 1991). However, these studies did not incorporate higher–order statistical details concerning the distribution of the component material particles, nor did they consider the most general linear scenario represented by bianisotropic HCMs.

In this paper we present the extended third–order SPFT for biansotropic HCMs which are weakly anisotropic, and investigate the convergence of the extended SPFT.

The following notation is used: Vector quantities are underlined. Double underlining and normal (bold) face signifies a 3×3 (6×6) dyadic. The inverse of a dyadic $\underline{\underline{\mathbf{M}}}$ is denoted by $\underline{\underline{\mathbf{M}}}^{-1}$. The 3×3 (6×6) identity dyadic is represented by $\underline{\underline{I}}$ ($\underline{\underline{\mathbf{I}}}$). All field–related quantities are implicitly functions of the angular frequency ω. The permittivity and permeability of free space are denoted as ϵ_0 and μ_0, respectively; the free–space wavenumber is $k_0 = \omega\sqrt{\epsilon_0\mu_0}$. The real and imaginary parts of $z \in \mathbb{C}$ are represented by $\mathrm{Re}\, z$ and $\mathrm{Im}\, z$, respectively. A compact representation of the constitutive parameters for the homogeneous bianisotropic material specified by the Tellegen constitutive relations

$$\left.\begin{array}{l} \underline{D}(\underline{r}) = \underline{\underline{\epsilon}} \bullet \underline{E}(\underline{r}) + \underline{\underline{\xi}} \bullet \underline{H}(\underline{r}) \\ \underline{B}(\underline{r}) = \underline{\underline{\zeta}} \bullet \underline{E}(\underline{r}) + \underline{\underline{\mu}} \bullet \underline{H}(\underline{r}) \end{array}\right\} \tag{1}$$

is provided by the 6×6 constitutive dyadic

$$\underline{\underline{\mathbf{K}}} = \left[\begin{array}{cc} \underline{\underline{\epsilon}} & \underline{\underline{\xi}} \\ \underline{\underline{\zeta}} & \underline{\underline{\mu}} \end{array} \right] . \tag{2}$$

Herein, $\underline{\underline{\epsilon}}$ and $\underline{\underline{\mu}}$ are the 3×3 permittivity and permeability dyadics , respectively, while $\underline{\underline{\xi}}$ and $\underline{\underline{\zeta}}$ are the 3×3 magnetoelectric dyadics. Subscripts on $\underline{\underline{\mathbf{K}}}$ identify the particular material that $\underline{\underline{\mathbf{K}}}$ describes.

2 Strong–property–fluctuation theory

2.1 Component materials

We consider the homogenization of two distinct material phases: phase a and phase b, both of which consist of spherical particles of average radius η. All space is taken to be partitioned into the disjoint regions V_a and V_b that contain the phases a and b, respectively. The phases a and b are randomly distributed, as specified by the characteristic functions

$$\Phi_\ell(\underline{r}) = \begin{cases} 1, & \underline{r} \in V_\ell \\ \\ 0, & \underline{r} \notin V_\ell \end{cases} , \qquad (\ell = a, b). \tag{3}$$

In particular, within the SPFT statistical moments of Φ_ℓ are utilized to characterize the component phase distributions. The volume fraction of phase ℓ is given by the first moment; i.e.,

$$\langle\, \Phi_\ell(\underline{r}) \,\rangle = f_\ell, \qquad (\ell = a, b); \tag{4}$$

and we have $f_a + f_b = 1$. The physically–motivated step function (Tsang, Kong, & Newton, 1982)

$$\langle\, \Phi_\ell(\underline{r})\, \Phi_\ell(\underline{r}')\, \rangle = \begin{cases} f_\ell, & |\, \underline{r} - \underline{r}'\, | \le L \\ \\ f_\ell^2, & |\, \underline{r} - \underline{r}'\, | > L \end{cases} , \qquad (\ell = a, b) \tag{5}$$

is often adopted as the second moment for the second–order SPFT. The correlation length L is required to be much smaller than the electromagnetic wavelength(s) but larger than the size of the component phase particles. It is worth noting that the second–order SPFT estimates of the HCM constitutive parameters have been found to be largely insensitive to the particular form of the second moment (Mackay, Lakhtakia, & Weiglhofer, 2001b). In keeping with (5), the third–order SPFT has been established for the third moment (Mackay, Lakhtakia, & Weiglhofer, 2001a)

$$\langle\, \Phi_\ell(\underline{r})\, \Phi_\ell(\underline{r}')\, \Phi_\ell(\underline{r}'')\, \rangle = \begin{cases} f_\ell^3, & \min\{L_{12}, L_{13}, L_{23}\} > L \\ \\ f_\ell, & \max\{L_{12}, L_{13}, L_{23}\} \le L \\ \\ \frac{1}{3}\,(f_\ell + 2 f_\ell^3), & \text{one of } L_{12}, L_{13}, L_{23} \le L \\ \\ \frac{1}{3}\,(2 f_\ell + f_\ell^3), & \text{two of } L_{12}, L_{13}, L_{23} \le L \end{cases} , \qquad (\ell = a, b)\,, \tag{6}$$

where

$$L_{12} = |\underline{r} - \underline{r}'|\,, \qquad L_{13} = |\underline{r} - \underline{r}''|\,, \qquad L_{23} = |\underline{r}' - \underline{r}''|\,. \tag{7}$$

The component material phases a and b are homogeneous materials, characterized by the 6×6 constitutive dyadics $\underline{\underline{\mathbf{K}}}_a$ and $\underline{\underline{\mathbf{K}}}_b$, respectively.

2.2 Homogenized composite material

The constitutive dyadic of the HCM, as estimated by the nth–order SPFT, is given by (Mackay, Lakhtakia, & Weiglhofer, 2000)

$$\underline{\underline{\mathbf{K}}}^{[n]}_{HCM} = \underline{\underline{\mathbf{K}}}_{cm} - \frac{1}{i\omega}\left[\underline{\underline{\mathbf{I}}} + \underline{\underline{\mathbf{\Sigma}}}^{[n]}(\eta, L) \cdot \underline{\underline{\mathbf{D}}}(\eta)\right]^{-1} \cdot \underline{\underline{\mathbf{\Sigma}}}^{[n]}(\eta, L). \tag{8}$$

Herein, the constitutive dyadic $\underline{\underline{\mathbf{K}}}_{cm}$ characterizes a comparison medium whose constitutive parameters are provided by the Bruggeman homogenization formalism.

The depolarization dyadic

$$\underline{\underline{\mathbf{D}}}(\eta) = \underline{\underline{\mathbf{D}}}^{0} + \underline{\underline{\mathbf{D}}}^{>0}(\eta) \tag{9}$$

has two parts (Cui & Mackay, 2007a): $\underline{\underline{\mathbf{D}}}^{0}$ represents the contribution to the depolarization arising from component particles in the limit $\eta \to 0$, whereas $\underline{\underline{\mathbf{D}}}^{>0}(\eta)$ represents the depolarization contribution arising from the nonzero volume of the component particles. Often in homogenization studies the $\underline{\underline{\mathbf{D}}}^{>0}(\eta)$ contribution is neglected, but recent studies have highlighted the significance of this contribution, particularly in the context of scattering losses (Cui & Mackay, 2007a,b). The conventional SPFT incorporates $\underline{\underline{\mathbf{D}}}^{0}$ only as the depolarization dyadic, whereas the extended SPFT accommodates both $\underline{\underline{\mathbf{D}}}^{0}$ and $\underline{\underline{\mathbf{D}}}^{>0}(\eta)$. The mathematical expressions for $\underline{\underline{\mathbf{D}}}^{0}$ and $\underline{\underline{\mathbf{D}}}^{>0}(\eta)$ are complicated, especially for bianisotropic HCMs, but integral representations are available which can be straightforwardly evaluated using standard numerical techniques (Press, Flannery, Teukolsky, & Vetterling, 1992). These integral representations are provided in the Appendix.

The mass operator term $\underline{\underline{\mathbf{\Sigma}}}^{[n]}(\eta, L)$ in (8) vanishes for the zeroth– and first–order versions of the SPFT (Tsang & Kong, 1981; Mackay, Lakhtakia, & Weiglhofer, 2000); i.e.,

$$\underline{\underline{\mathbf{\Sigma}}}^{[0]} = \underline{\underline{\mathbf{\Sigma}}}^{[1]} = \underline{\underline{\mathbf{0}}}. \tag{10}$$

By implementing the two–point covariance function (5), the second–order mass operator term is given by (Mackay, Lakhtakia, & Weiglhofer, 2000)

$$\underline{\underline{\mathbf{\Sigma}}}^{[2]}(\eta, L) = f_a f_b \left[\underline{\underline{\boldsymbol{\chi}}}_a(\eta) - \underline{\underline{\boldsymbol{\chi}}}_b(\eta)\right] \cdot \underline{\underline{\mathbf{D}}}^{>0}(L) \cdot \left[\underline{\underline{\boldsymbol{\chi}}}_a(\eta) - \underline{\underline{\boldsymbol{\chi}}}_b(\eta)\right], \tag{11}$$

with the polarizability density dyadics

$$\underline{\underline{\boldsymbol{\chi}}}_\ell(\eta) = -i\omega\left(\underline{\underline{\mathbf{K}}}_\ell - \underline{\underline{\mathbf{K}}}_{cm}\right) \cdot \left[\underline{\underline{\mathbf{I}}} + i\omega\underline{\underline{\mathbf{D}}}(\eta) \cdot \left(\underline{\underline{\mathbf{K}}}_\ell - \underline{\underline{\mathbf{K}}}_{cm}\right)\right]^{-1}, \qquad (\ell = a, b). \tag{12}$$

The three–point covariance function (6) yields the third–order mass operator term (Mackay, Lakhtakia, & Weiglhofer, 2001a)

$$\begin{aligned}\underline{\underline{\mathbf{\Sigma}}}^{[3]}(\eta, L) = \underline{\underline{\mathbf{\Sigma}}}^{[2]}(\eta, L) + \frac{f_a(1-2f_a)}{3(1-f_a)^2}\underline{\underline{\boldsymbol{\chi}}}_a(\eta) \cdot \Big[\underline{\underline{\mathbf{V}}}(\eta) \cdot \underline{\underline{\boldsymbol{\chi}}}_a(\eta) \cdot \underline{\underline{\mathbf{D}}}^{>0}(L) \\ + \underline{\underline{\mathbf{D}}}^{>0}(L) \cdot \underline{\underline{\boldsymbol{\chi}}}_a(\eta) \cdot \underline{\underline{\mathbf{V}}}(\eta) + \underline{\underline{\mathbf{D}}}^{>0}(L) \cdot \underline{\underline{\boldsymbol{\chi}}}_a(\eta) \cdot \underline{\underline{\mathbf{D}}}^{>0}(L)\Big] \cdot \underline{\underline{\boldsymbol{\chi}}}_a(\eta),\end{aligned} \tag{13}$$

where

$$\underline{\underline{\mathbf{V}}}(\eta) = \frac{1}{i\omega}\,\underline{\underline{\mathbf{K}}}_{cm}^{-1} - \underline{\underline{\mathbf{D}}}(\eta). \tag{14}$$

3 Numerical studies

We now apply the extended third–order SPFT presented in §2 to a specific bianisotropic homogenization scenario. As an illustrative example, let us consider the homogenization of (i) a magnetically–biased ferrite medium described by the constitutive dyadic (Lax & Button, 1962; Collin, 1966)

$$\underline{\underline{\mathbf{K}}}_a = \delta \left[\begin{array}{cc} \epsilon_0\,\epsilon_a\,\underline{\underline{I}} & \underline{\underline{0}} \\ \underline{\underline{0}} & \mu_0 \left(\begin{array}{ccc} \mu_a^x & i\mu_a^g & 0 \\ -i\mu_a^g & \mu_a^x & 0 \\ 0 & 0 & \mu_a^z \end{array} \right) \end{array} \right] \tag{15}$$

and (ii) an isotropic chiral medium described by the constitutive dyadic (Lakhtakia, 1994)

$$\underline{\underline{\mathbf{K}}}_b = \left[\begin{array}{cc} \epsilon_0\epsilon_b\,\underline{\underline{I}} & i\sqrt{\epsilon_0\mu_0}\,\xi_b\,\underline{\underline{I}} \\ -i\sqrt{\epsilon_0\mu_0}\,\xi_b\,\underline{\underline{I}} & \mu_0\mu_b\,\underline{\underline{I}} \end{array} \right]. \tag{16}$$

The parameter δ in (15) provides a means of varying the constitutive contrast between the component material phases. The constitutive relations of the resulting HCM — which is known as a Faraday chiral medium — are rigorously established (Engheta, Jaggard, & Kowarz, 1992; Weiglhofer & Lakhtakia, 1998). The constitutive dyadic of the HCM, as estimated by the nth order SPFT, has the general form

$$\underline{\underline{\mathbf{K}}}_{HCM}^{[n]} = \left[\begin{array}{cc} \epsilon_0 \left(\begin{array}{ccc} \epsilon_{HCM}^x & i\epsilon_{HCM}^g & 0 \\ -i\epsilon_{HCM}^g & \epsilon_{HCM}^x & 0 \\ 0 & 0 & \epsilon_{HCM}^z \end{array} \right) & i\sqrt{\epsilon_0\mu_0} \left(\begin{array}{ccc} \xi_{HCM}^x & i\xi_{HCM}^g & 0 \\ -i\xi_{HCM}^g & \xi_{HCM}^x & 0 \\ 0 & 0 & \xi_{HCM}^z \end{array} \right) \\ -i\sqrt{\epsilon_0\mu_0} \left(\begin{array}{ccc} \xi_{HCM}^x & i\xi_{HCM}^g & 0 \\ -i\xi_{HCM}^g & \xi_{HCM}^x & 0 \\ 0 & 0 & \xi_{HCM}^z \end{array} \right) & \mu_0 \left(\begin{array}{ccc} \mu_{HCM}^x & i\mu_{HCM}^g & 0 \\ -i\mu_{HCM}^g & \mu_{HCM}^x & 0 \\ 0 & 0 & \mu_{HCM}^z \end{array} \right) \end{array} \right]. \tag{17}$$

An HCM of the same form also arises from the homogenization of a magnetically–biased plasma and an isotropic chiral medium (Weiglhofer, Lakhtakia, & Michel, 1998; Weiglhofer & Mackay, 2000). Bearing in mind that the third–order SPFT is established only for bianisotropic mediums which are weakly anisotropic (Mackay, Lakhtakia, & Weiglhofer, 2001a), we select the following representative values for the constitutive parameters of the component material phases: $\epsilon_a = 1.2 + i0.02$, $\mu_a^x = 3.5 + i0.08$, $\mu_a^g = 0.7 + i0.005$, $\mu_a^z = 3.0 + i0.06$; $\epsilon_b = 2.5 + i0.1$, $\xi_b = 1 + i0.07$ and $\mu_b = 1.75 + i0.09$. Results which are qualitatively similar to those presented here were observed — in further studies not reported here — when different values were selected for the constitutive parameters of the component materials.

In the following numerical studies, the correlation length L is fixed[3] for each value of δ considered, while the particle size parameter η varies from 0 to $L/2$. In order to conform to the long–wavelength regime under which the SPFT estimates of the HCM parameters are derived, the value of L is selected such that the scalar $Q \ll 1$, where

$$Q = \frac{\max\,\{|\gamma_1|,\,|\gamma_2|,\,|\gamma_3|,\,|\gamma_4|\}}{2\pi}\,L, \tag{18}$$

with $\{\gamma_i \,|\, i = 1, \ldots, 4\}$ being the four independent wavenumbers supported by the HCM. For simplicity, we choose the wavenumbers associated with propagation along the Cartesian z axis (Mackay & Lakhtakia, 2004); i.e.,

$$\left.\begin{array}{l}
\gamma_1 = k_0 \left(\sqrt{\epsilon^x_{HCM} + \epsilon^g_{HCM}} \sqrt{\mu^x_{HCM} + \mu^g_{HCM}} - \xi^x_{HCM} - \xi^g_{HCM} \right) \\
\gamma_2 = k_0 \left(-\sqrt{\epsilon^x_{HCM} + \epsilon^g_{HCM}} \sqrt{\mu^x_{HCM} + \mu^g_{HCM}} - \xi^x_{HCM} - \xi^g_{HCM} \right) \\
\gamma_3 = k_0 \left(\sqrt{\epsilon^x_{HCM} - \epsilon^g_{HCM}} \sqrt{\mu^x_{HCM} - \mu^g_{HCM}} + \xi^x_{HCM} - \xi^g_{HCM} \right) \\
\gamma_4 = k_0 \left(-\sqrt{\epsilon^x_{HCM} - \epsilon^g_{HCM}} \sqrt{\mu^x_{HCM} - \mu^g_{HCM}} + \xi^x_{HCM} - \xi^g_{HCM} \right)
\end{array}\right\}. \tag{19}$$

All numerical calculations were carried out using an angular frequency $\omega = 2\pi \times 10^{10}$ rad s^{-1} with the volume fraction fixed at $f_a = 0.3$.

The zeroth–, second– and third–order SPFT estimates of the HCM constitutive parameters μ^x_{HCM}, μ^g_{HCM} and μ^z_{HCM} are plotted against the size parameter η in Figure 1 for the case where $\delta = 10$. Here, the correlation length is set at $L = 0.45$ mm, in order that $Q = 0.1$ at $\eta = L/2$. The third–order estimates of the real and imaginary parts of μ^x_{HCM}, μ^g_{HCM} and μ^z_{HCM} increase steadily as η is increased, as do the zeroth–order and second–order estimates, but the difference between the third–order estimates and the second–order estimates remains very small for all values of η. In contrast, there are plainly significant differences between the second–order and zeroth–order estimates. Furthermore, the difference between the zeroth– and second–order estimates increases in magnitude slightly as the the size parameter η increases. The corresponding graphs for the permittivity and magnetoelectric constitutive parameters of the HCM are qualitatively similar to those graphs presented in Figure 1. Accordingly, these are not displayed here.

Plots of μ^x_{HCM}, μ^g_{HCM} and μ^z_{HCM} versus η for the case where $\delta = 30$ are shown in Figure 2. The correlation length $L = 0.28$ mm was used for the calculations of Figure 2, thereby resulting in $Q = 0.1$ at $\eta = L/2$. As is the case for $\delta = 10$, the second–order estimates are plainly different to the zeroth–order estimates for $\delta = 30$. The differences between second–order and third–order estimates of the real and imaginary parts of the HCM constitutive parameters increase slightly as δ increases, but they remain small for all values of η. The corresponding permittivity and magnetoelectric constitutive parameters of the HCM exhibit trends which are qualitatively similar to those shown in Figure 2 for the HCM magnetic constitutive parameters.

[3]This applies to the second–order and third–order SPFT calculations; L does not feature in the zeroth–order SPFT.

4 Concluding remarks

It is demonstrated by our numerical studies in §3 (and in further studies not presented here) that the extended SPFT at the third–order level of approximation does not add significantly to the HCM estimates yielded by the second–order extended SPFT. The differences between second–order and third–order estimates of the HCM constitutive parameters are very small for all values of the size parameter investigated, even when the constitutive contrast between the component materials is as large as a factor of 30. Significant differences between the second– and third–order estimates arise only when (i) the correlation length and/or size parameter become similar in magnitude to the electromagnetic wavelength(s); and/or (ii) the constitutive contrast between the component materials becomes enormous. In the case of (i) the bounds imposed by the long–wavelength regime are exceeded, while in the case of (ii) the contrast between the polarizability density dyadics $\underline{\underline{\boldsymbol{\chi}}}_a$ and $\underline{\underline{\boldsymbol{\chi}}}_b$ is likely to become strong. In either scenario the basic assumptions underlying the long–wavelength SPFT are violated (Mackay, Lakhtakia, & Weiglhofer, 2000, 2001a). We therefore conclude that the extended SPFT converges at the second–order level of approximation for bianisotropic HCMs which are weakly anisotropic.

Acknowledgement: JC is supported by a *Scottish Power–EPSRC Dorothy Hodgkin Postgraduate Award*. TGM is supported by a *Royal Society of Edinburgh/Scottish Executive Support Research Fellowship*.

Appendix

The depolarization dyadic $\underline{\underline{\mathbf{D}}}(\eta)$, as specified by (9), for a spherical inclusion of radius η, immersed in a bianisotropic comparison medium described by the constitutive dyadic $\underline{\underline{\mathbf{K}}}_{cm}$, is derived from the dyadic Green function of the comparison medium. The contribution associated with $\eta \to 0$ is provided by the η–independent surface integral (Michel, 1997; Michel & Weiglhofer, 1997)

$$\underline{\underline{\mathbf{D}}}^0 = \frac{1}{4\pi i\omega} \int_{\phi=0}^{2\pi} \int_{\theta=0}^{\pi} \underline{\underline{\mathbf{B}}}_{cm}(\hat{\underline{q}}) \;\; \sin\theta \; d\theta \; d\phi, \tag{20}$$

with dyadic integrand

$$\underline{\underline{\mathbf{B}}}_{cm}(\hat{\underline{q}}) \;\; = \;\; \frac{1}{b(\theta,\phi)} \left[\begin{array}{cc} \alpha_\mu(\theta,\phi)\, \hat{\underline{q}}\,\hat{\underline{q}} & -\alpha_\zeta(\theta,\phi)\, \hat{\underline{q}}\,\hat{\underline{q}} \\ -\alpha_\xi(\theta,\phi)\, \hat{\underline{q}}\,\hat{\underline{q}} & \alpha_\epsilon(\theta,\phi)\, \hat{\underline{q}}\,\hat{\underline{q}} \end{array} \right]. \tag{21}$$

Herein the scalars

$$\alpha_P(\theta,\phi) = \hat{\underline{q}} \bullet \underline{\underline{P}}_{cm} \bullet \hat{\underline{q}}\,, \qquad\qquad (P = \epsilon, \zeta, \xi, \mu) \tag{22}$$

and

$$b(\theta,\phi) = \left[\alpha_\epsilon(\theta,\phi)\, \alpha_\mu(\theta,\phi)\right] - \left[\alpha_\xi(\theta,\phi)\, \alpha_\zeta(\theta,\phi)\right], \tag{23}$$

while $\hat{\underline{q}}$ is the radial unit vector specified by the spherical coordinates θ and ϕ.

The depolarization contribution associated with the nonzero inclusion volume is given by the η–dependent volume integral (Mackay, 2004; Cui & Mackay, 2007a)

$$\underline{\underline{\mathbf{D}}}^{>0}(\eta) = \frac{\eta}{2\pi^2 i\omega} \int_{\underline{q}} \frac{1}{q^2} \left[\frac{\sin(q\eta)}{q\eta} - \cos(q\eta) \right] \left[\underline{\underline{\mathbf{A}}}_{cm}^{-1}(\underline{q}) - \underline{\underline{\mathbf{B}}}_{cm}(\hat{\underline{q}}) \right] \, d^3\underline{q}, \tag{24}$$

wherein

$$\underline{\underline{\mathbf{A}}}_{cm}(\underline{q}) = \left[\begin{array}{cc} \underline{\underline{0}} & (\underline{q}/\omega) \times \underline{\underline{I}} \\ -(\underline{q}/\omega) \times \underline{\underline{I}} & \underline{\underline{0}} \end{array} \right] + \underline{\underline{\mathbf{K}}}_{cm}. \tag{25}$$

The depolarization integrals (20) and (24) are straightforwardly evaluated using standard numerical techniques (Press, Flannery, Teukolsky, & Vetterling, 1992).

References

[1] Collin, R.E. 1966. *Foundations for microwave engineering*. New York: McGraw–Hill.

[2] Cui, J., & T.G. Mackay. 2007a. Depolarization regions of nonzero volume in bianisotropic homogenized composites. *Waves Random Complex Media* (in press).

[3] Cui, J., & T.G. Mackay. 2007b. Depolarization regions of nonzero volume for anisotropic, cubically nonlinear, homogenized nanocomposites. *J. Nanophotonics* 1:013506.

[4] Doyle, W.T. 1989. Optical properties of a suspension of metal spheres. *Phys. Rev. B* 39:9852–9858.

[5] Dungey, C.E., & C.F. Bohren. 1991. Light scattering by nonspherical particles: a refinement to the coupled–dipole method. *J. Opt. Soc. Am. A* 8:81–87.

[6] Engheta, N., D.L. Jaggard, & M.W. Kowarz. 1992. Electromagnetic waves in Faraday chiral media. *IEEE Trans. Antennas Propagat.* 40:367–374.

[7] Genchev, Z.D. 1992. Anisotropic and gyrotropic version of Polder and van Santen's mixing formula. *Waves Random Media* 2:99–110.

[8] Lakhtakia, A. 1994. *Beltrami fields in chiral media*. World Scientific: Singapore.

[9] Lakhtakia, A., ed. 1996. *Selected papers on linear optical composite materials*. Bellingham, WA: SPIE Optical Engineering Press.

[10] Lakhtakia, A. 2001. Application of strong permittivity fluctuation theory for isotropic, cubically nonlinear, composite mediums. *Opt. Commun.* 192:145–151.

[11] Lakhtakia, A., & B. Shanker. 1993. Beltrami fields within continuous source regions, volume integral equations, scattering algorithms, and the extended Maxwell-Garnett model. *Int. J. Appl. Electromag. in Mater.* 4:65–82.

[12] Lax, B., & K.J. Button. 1962. *Microwave ferrites and ferrimagnetics*. New York: McGraw–Hill.

[13] Mackay, T.G. 2003. Geometrically derived anisotropy in cubically nonlinear dielectric composites. *J. Phys. D: Appl. Phys.* 36:583–591.

[14] Mackay, T.G. 2004. Depolarization volume and correlation length in the homogenization of anisotropic dielectric composites. *Waves Random Media* 14: 485–498; erratum: *Waves Random Complex Media* 16: 85 (2006).

[15] Mackay, T.G. 2005. Linear and nonlinear homogenized composite mediums as metamaterials. *Electromagnetics* 25:461–481.

[16] Mackay, T.G., & A. Lakhtakia. 2004. Plane waves with negative phase velocity in Faraday chiral mediums. *Phys. Rev. E* 69:026602.

[17] Mackay, T.G., A. Lakhtakia, & W.S. Weiglhofer. 2000. Strong–property–fluctuation theory for homogenization of bianisotropic composites: formulation. *Phys. Rev. E* 62:6052–6064; erratum: 63:049901 (2001).

[18] Mackay, T.G., A. Lakhtakia, & W.S. Weiglhofer. 2001a. Third–order implementation and convergence of the strong–property–fluctuation theory in electromagnetic homogenization. *Phys. Rev. E* 64:066616.

[19] Mackay, T.G., A. Lakhtakia, & W.S. Weiglhofer. 2001b. Homogenisation of similarly oriented, metallic, ellipsoidal inclusions using the bilocal–approximated strong–property–fluctuation theory. *Opt. Commun.* 197:89–95.

[20] Mackay, T.G., A. Lakhtakia, & W.S. Weiglhofer. 2003. The strong–property–fluctuation theory for cubically nonlinear, isotropic chiral composite mediums. *Electromagnetics* 23:455–479.

[21] Michel, B. 1997. A Fourier space approach to the pointwise singularity of an anisotropic dielectric medium. *Int. J. Appl. Electromagn. Mech.* 8:219–227.

[22] Michel, B., & A. Lakhtakia. 1995. Strong–property–fluctuation theory for homogenizing chiral particulate composites. *Phys. Rev. E* 51:5701–5707.

[23] Michel, B., & W.S. Weiglhofer. 1997. Pointwise singularity of dyadic Green function in a general bianisotropic medium. *Arch. Elektr. Übertrag.* 51:219–223; erratum: 52:310 (1998).

[24] Press, W.H., B.P. Flannery, S.A. Teukolsky, & W.T. Vetterling. 1992. *Numerical Recipes in Fortran*, 2nd. ed. Cambridge, UK: Cambridge University Press.

[25] Prinkey, M.T., A. Lakhtakia, & B. Shanker. 1994. On the extended Maxwell–Garnett and the extended Bruggeman approaches for dielectric-in-dielectric composites *Optik* 96:25–30.

[26] Shanker, B. 1996. The extended Bruggeman approach for chiral–in–chiral mixtures. *J. Phys. D: Appl. Phys.* 29:281–288.

[27] Shanker, B., & A. Lakhtakia. 1993a. Extended Maxwell Garnett model for chiral–in–chiral composites. *J. Phys. D: Appl. Phys.* 26:1746–1758.

[28] Shanker, B., & A. Lakhtakia. 1993b. Extended Maxwell Garnett formalism for composite adhesives for microwave-assisted adhesion of polymer surfaces. *J. Composite Mater.* 27:1203–1213.

[29] Tsang, L., & J.A. Kong. 1981. Scattering of electromagnetic waves from random media with strong permittivity fluctuations. *Radio Sci.* 16:303–320.

[30] Tsang, L, J.A. Kong, & R.W. Newton. 1982. Application of strong fluctuation random medium theory to scattering of electromagnetic waves from a half–space of dielectric mixture. *IEEE Trans. Antennas Propagat.* 30: 292–302.

[31] Walser, R.M. 2003. Metamaterials: an introduction. In *Introduction to complex mediums for optics and electromagnetics*, ed. W.S. Weiglhofer and A. Lakhtakia. Bellingham, WA: SPIE Press.

[32] Ward, L. 1995. *The optical constants of bulk materials and films*, 2nd ed. Bristol, UK: Adam Hilger.

[33] Weiglhofer, W.S., & A. Lakhtakia. 1998. The correct constitutive relations of chiroplasmas and chiroferrites. *Microw. Opt. Technol. Lett.* 17:405–408.

[34] Weiglhofer, W.S., A. Lakhtakia, & B. Michel. 1998. On the constitutive parameters of a chiroferrite composite medium. *Microwave Opt. Technol. Lett.* 18:342–345.

[35] Weiglhofer, W.S., & T.G. Mackay. 2000. Numerical studies of the constitutive parameters of a chiroplasma composite medium. *Arch. Elektr. Übertrag.* 54:259–265.

[36] Zhuck, N.P. 1994. Strong–fluctuation theory for a mean electromagnetic field in a statistically homogeneous random medium with arbitrary anisotropy of electrical and statistical properties. *Phys. Rev. B* 50:15636–15645.

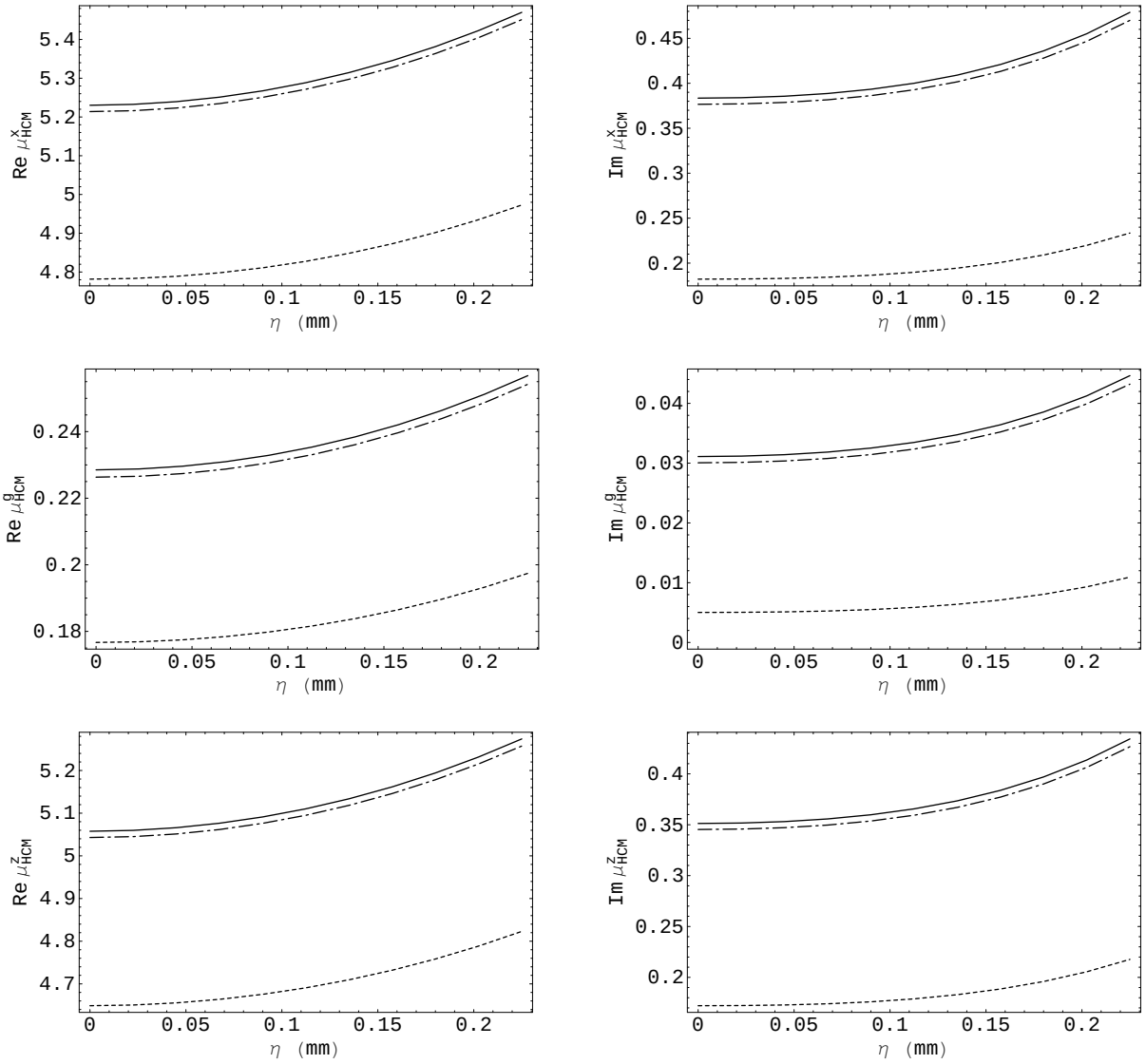

Figure 1: Real (left) and imaginary (right) parts of the HCM constitutive parameters $\mu^{x,z,g}_{HCM}$ plotted against η (mm) for $\delta = 10$. Key: dashed curve is the zeroth–order SPFT estimate; broken dashed curve is the second–order SPFT estimate; and solid curve is the third–order SPFT estimate.

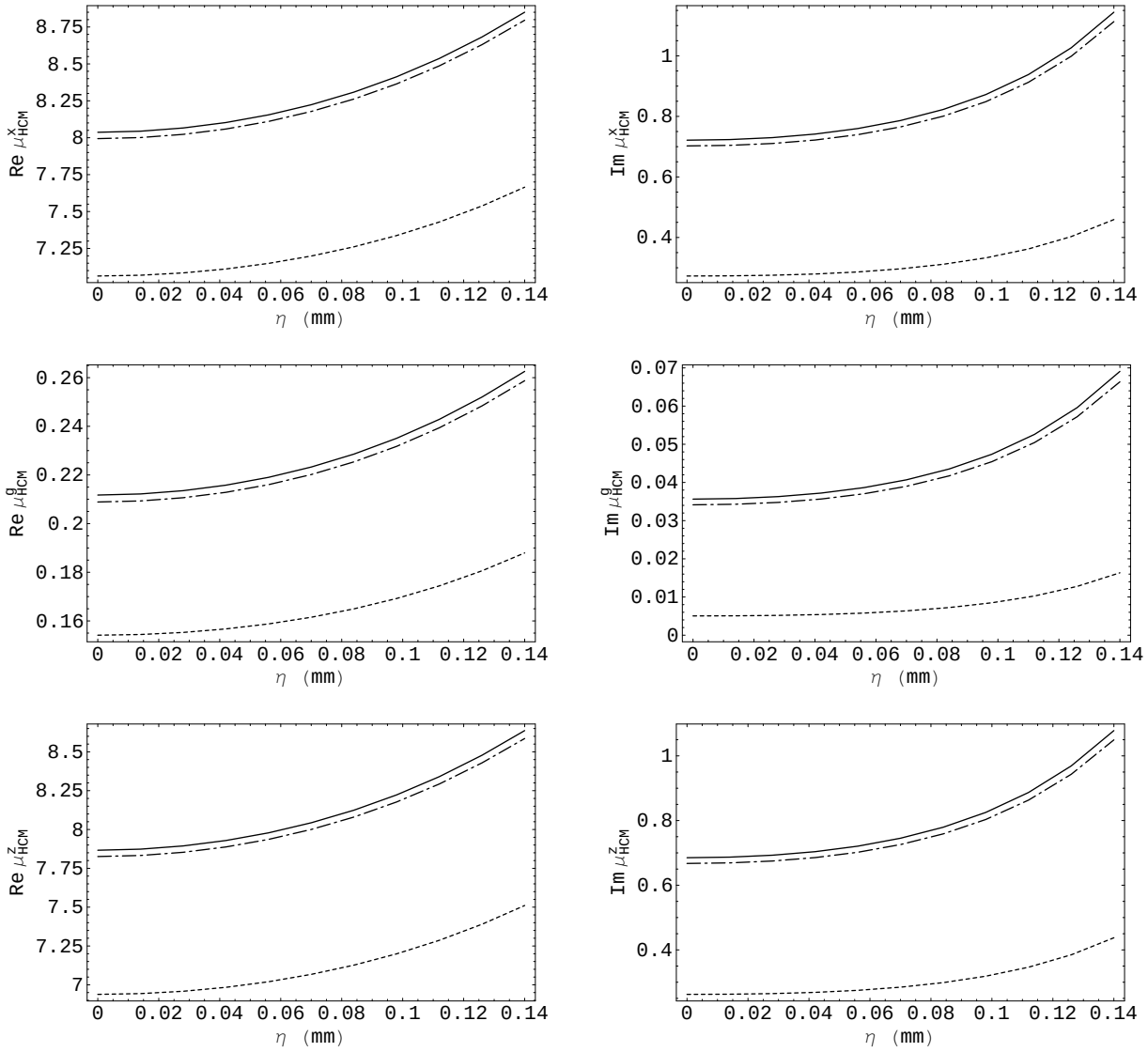

Figure 2: As Figure 1 but for $\delta = 30$.